Full-Wave Analysis of Cavity-Backed and Probe-Fed Microstrip Patch Arrays by a Hybrid Mode-Matching Generalized Scattering Matrix and Finite-Element Method

Miguel A. González de Aza, José A. Encinar, *Member, IEEE*, Juan Zapata, *Member, IEEE*, and Manuel Lambea, *Member, IEEE*

***Abstract*— A full-wave method to analyze probe-fed infinite phased arrays of arbitrarily shaped microstrip patches residing in a cavity is proposed. The method is based on a combination of the mode matching and finite-element methods (MM-FEM) and provides a rigorous characterization of the coaxial feed. The radiated field to the half space is expressed as a Floquet's harmonic expansion reducing the analysis to a single elementary cell of the periodic antenna. The unit cell is analyzed as an open-ended succession of homogeneous waveguides of diverse cross sections. Each transition between waveguides is solved by a hybrid MM-FEM procedure to obtain its generalized scattering matrix (GSM). Finally, the GSM of the structure, which characterizes the array, is obtained from the individual GSM's by a cascading process. The method is also extended to the analysis of conventional probe-fed microstrip arrays by using the waveguide simulator model. Several prototypes, implemented and measured in waveguide simulator, have been analyzed to prove the validity and efficiency of the proposed method.**

***Index Terms*— Finite-element methods, microstrip arrays, mode-matching, scattering matrices.**

I. Introduction

THE attractive advantages of the microstrip antennas are widely known, as well as their increasing number of applications [1]. However, they possess intrinsic limitations as the narrow impedance bandwidth or the excitation of the surface waves. A straightforward and effective means of improving the bandwidth performance is to employ thick substrates between the microstrip antenna and the ground plane or to add parasitic stacked patches. However, as the substrate becomes thicker, the surface waves generation rises. In the case of arrays, the mutual coupling between elements also increases and it is more difficult to obtain a good impedance matching between the radiant elements and the feed lines as the array is scanned. In addition, scan blindness may occur in large arrays. In the last years, a method of preventing surface wave modes by insertion of metallic baffles between the patch elements has been investigated [2]–[5]. Microstrip patch arrays residing in a cavity allow to use thicker substrates without the limitation in the scanning range [2]. To analyze these structures simple approaches become inefficient and full-wave analyses are required such as integral-equation (IE) formulation [2], finite-element method (FEM) [3], or hybrid techniques [4]–[6].

On the other hand, for coaxially fed microstrip antennas, a rigorous modeling of the excitation is also required, both for conventional and cavity-backed patches, particularly when these are printed on thick dielectric substrates or when the size of the probe and coaxial aperture are not negligible. Simplified models of the probe coaxial feed based on a current filament [4], [7] (only applicable to thin substrates) and a finite width surface current [2], [3] are commonly employed. However, with these simplifications the current variations and the probe radius are not taking into account. A more precise model proposed in [8] and [9] includes the effect of the probe by using an additional attachment mode, derived from the corresponding cavity model solution, although the coaxial aperture on the ground plane is not considered. Other formulation for the attachment mode has been proposed in [10] with a more rigorous model consisting of imposing also a magnetic current on the aperture. However, it does not take into account the alteration of the aperture fields. To include the effect of the probe radius, the cavity model has been employed with magnetic walls [11] or boundary admittances at the edges [12]. The mode-matching (MM) technique is used in [11] to analyze the junction cavity-coaxial probe, but it is only valid for canonical geometries, moderate thick substrates, and isolated radiant elements.

Purely numerical techniques such as the finite-difference time-domain (FDTD) method [13] have been used to analyze more rigorously the excitation, but they show others limitations such as the employ of very fine meshes for an accurate probe modeling and tri-dimensional meshing with suitable boundary conditions. In the context of three-dimensional (3-D) FEM, complex feed-modeling procedures with similar computation time and storage limitations have also been proposed [5], [6].

In this paper, we present a full-wave method for the analysis of probe-fed infinite phased arrays of arbitrarily shaped microstrip patches residing in a cavity that provides an accurate modeling of the coaxial feed. It is based on a hybrid numerical procedure that combines the MM, generalized scattering ma-

Manuscript received March 11, 1997; revised August 14, 1997.

The authors are with the Departamento de Electromagnetismo y Teoría de Circuitos, E.T.S.I. de Telecomunicación, Universidad Politécnica de Madrid, Ciudad Universitaria s/n, Madrid, 28040 Spain.

Publisher Item Identifier S 0018-926X(98)01492-6.

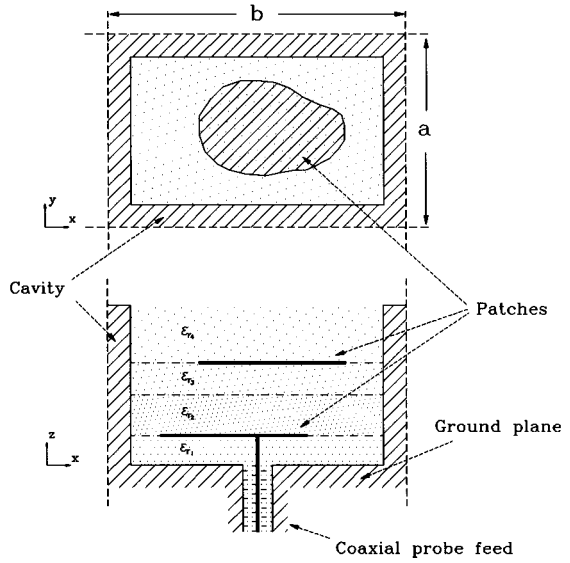

Fig. 1. Unit cell of a multilayer microstrip array of arbitrarily shaped stacked patches with probe feed and backed by rectangular cavities.

trix (GSM) techniques, and the two-dimensional (2-D) FEM. In the next section, the description of this method is accomplished. The procedure is extended and applied in Section III to the analysis of infinite arrays of conventional probe-fed microstrip patches by using the waveguide simulator model. Section IV contains input impedance and scan performance results for cavity-backed patch arrays and comparisons with measurements and other numerical predictions.

II. Analysis Method

A general problem of a multilayer microstrip array of arbitrarily shaped patches in stacked configuration, backed by rectangular cavities, and probe-fed by the center conductor of a coaxial transmission line is considered. The unit cell geometry of the periodic array is depicted in Fig. 1. The patches, cavities, and ground plane are assumed perfect conductors. The infinite array approach is assumed so that the periodic symmetry of the structure allows to use the Floquet's theorem in order to limit the analysis to a single element in a unit cell. The analysis method is based on the consideration of the elementary cell as an open-ended succession of homogeneous waveguides of diverse cross sections, with the same direction of propagation (z axis), radiating into half-space. The procedure is divided into two connected blocks: a multistepped waveguide structure and a transition between an infinite array of rectangular apertures and the free half-space. In the following subsections, the procedures to analyze these blocks are described.

A. Analysis of the Elementary Cell by Cascading GSM's

The elementary cell, excluding the rectangular aperture problem, is divided into simple discontinuities between homogeneous waveguides of different cross sections. The MM technique is applied to solve each individual transition using a modal representation for the fields, either analytical or numerical, in each side of the discontinuity i and j. Matching the electric and magnetic tangential field components by means of a Galerkin testing procedure and after some algebraic manipulations results in the GSM of the discontinuity

$$\begin{bmatrix} B^i \\ B^j \end{bmatrix} = \begin{bmatrix} S_{11} & S_{12} \\ S_{21} & S_{22} \end{bmatrix} \begin{bmatrix} A^i \\ A^j \end{bmatrix} \tag{1}$$

where A^i, B^i, A^j, and B^j are column matrices containing complex amplitudes of incident (A) and scattered (B) modes to/from the discontinuity in the i and j waveguide sections. The expressions used to obtain the submatrices S_{ij} in (1)

$$\begin{aligned} S_{21} &= 2[X(D^i)^{-1}X^t + D^j]^{-1}X \\ S_{22} &= [X(D^i)^{-1}X^t + D^j]^{-1}[D^j - X(D^i)^{-1}X^t] \\ S_{11} &= (D^i)^{-1}X^t S_{21} - I \\ S_{12} &= (D^i)^{-1}X^t(I + S_{22}) \end{aligned} \tag{2}$$

require the previous computation of the related MM-field coupling integral matrix, X, and the diagonal complex power matrices D^i and D^j. I is the identity matrix. The elements of X are

$$X(n,m) = \int_{S_c} (\vec{e}_n^{\,j} \times \vec{h}_m^{\,i})\, d\vec{s}. \tag{3}$$

The integral is defined over the common cross section S_c of the implicated waveguides and $\vec{e}_n^{\,j}$ and $\vec{h}_m^{\,i}$ are the normalized transversal components of the electric and magnetic field of the nth and mth modes in the j and i waveguides, respectively. The elements of D^i and D^j are

$$D^r(n) = \int_{S_r} (\vec{e}_n^{\,r} \times \vec{h}_n^{\,r})\, d\vec{s}, \qquad r = i, j \tag{4}$$

where S_r is the section of the r waveguide.

For canonical regions, as the coaxial line or the rectangular waveguide corresponding to the dielectric layers above the fed patch, the transversal mode components are derived analytically. However, waveguides without or with complicated analytical solution (as the transmission lines associated to the substrate with probe or to the patch geometry) are characterized numerically. In this case, the FEM is employed as described in Section II-B. A cascade connection process for the GSM's of the different discontinuities leads to the GSM of the first considered block.

B. MM at Interfaces with Noncanonical Waveguides

The analysis of discontinuities that involve homogeneous waveguides of arbitrary cross section is performed by a hybrid MM-FE procedure developed previously [14] and [15]. The technique requires the numerical computation of the modes for the noncanonical waveguides. The FEM is applied to the discretization of the appropriate functionals using a Galerkin procedure. The axial field components for TE and TM modes and the scalar electric potential for TEM modes are computed in the nodes of a mesh performed on the waveguide cross sections. Next, MM is applied to obtain the GSM of the considered discontinuity computing numerically the integrals (3) and (4) from the FE solution. This step is performed in an efficient way by using perfectly overlapped meshes for the waveguides in the FE implementation. This procedure will

allow to obtain the integrals $X(n,m)$ over the total common section as a summation of elemental integrals on each of the L finite elements S_{c_l}, which compose the mesh of S_c

$$X(n,m) = \sum_{l=1}^{L} \int_{S_{c_l}} (\vec{e}_n^{\,j} \times \vec{h}_m^{\,i})\, d\vec{s} \tag{5}$$

D^r is also computed as a summation of elemental integrals on S_r. More details about the computation of this coefficients are given in the Appendix.

For interfaces between canonical and noncanonical waveguides, both numerical and analytical modes may be employed. In contrast to other works, the FEM is only applied to compute numerical modes in noncanonical regions. Moreover, an appropriate field normalization leads to a frequency-independent internal product computation, allowing an efficient analysis over a wide bandwidth.

C. Interface: Array of Apertures-Free Half Space

The GSM computation of the interface—array of rectangular apertures half space—has also been accomplished by the MM method developed previously [16]. The technique is analogous to the standard MM procedure for waveguide discontinuities, but in this case, the fields in the half space are expressed as a Floquet's harmonic expansion and the analytical modal representation is used for the rectangular waveguide. The enforcement of the continuity condition on tangential electric and magnetic fields over the interface plane and the application of orthogonality properties of harmonics in the half space and modes in the waveguide allows us to obtain the GSM of the transition. Now, the field-coupling integral matrix (3) is composed of expressions that relate space harmonics and modes and are computed analytically over the aperture surface. A^i, B^i, and A^j, B^j in (1) are column matrices of complex coefficients of the rectangular waveguide modes and space harmonics, respectively.

The full-wave procedure is also applicable to arrays with arbitrarily shaped cavities since the modes in each region are computed numerically by FEM. In this case, the aperture array half-space transition is fragmented in two fictitious discontinuities by inserting an imaginary rectangular waveguide of zero length between the real cavity and the half space, as described in [17].

D. The Solution of the Overall Structure

A cascade connection process for the GSM's of the multistepped and the aperture problems, obtained as described in Sections II-B and C, respectively, provides the GSM of the overall structure, which relates modes in the coaxial line and Floquet's harmonics in the half space. The reflection coefficient for the TEM mode in the coaxial line S_{11} gives the active reflection coefficient of the infinite array. From the Floquet's harmonics coefficients, the field distribution on the aperture is directly obtained and, from this, the radiation patterns of the array. Thus, a full-wave analysis of the coaxial feed for infinite microstrip arrays residing in a cavity is performed, and an accurate prediction of the active input impedance is possible.

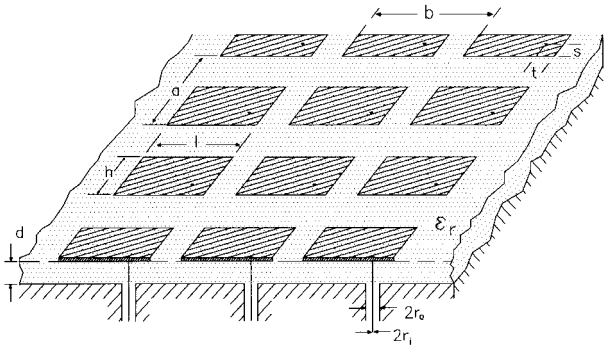

Fig. 2. Conventional infinite array of probe-fed rectangular microstrip patches ($a = b = 10$ cm; $l = 6$ cm; $h = 4$ cm; $s = t = 1$ cm; $\epsilon_r = 4.32$; $d = 0.8$ mm; coaxial feed: $\epsilon_{rx} = 1.951$; $r_i = 0.64$ mm; $r_o = 2.05$ mm).

The technique takes into account the real thickness of the metallizations and will be applicable to patches with arbitrary shape because this region is considered as a short length of an irregular shaped transmission line. Moreover, it will allow the inclusion of stacked patches and several dielectric layers by considering suitable waveguide or transmission line sections.

The scan performance array may be characterized by the normalized active element pattern $G(\theta,\varphi)$ or the active reflection coefficient. Both are related for a lossless array when no grating lobes are present in the visible range by $G(\theta,\varphi) = (1 - |S_{11}(\theta,\varphi)|^2)\cos\theta$, as described in [18].

III. Results of an Array in a Waveguide Simulator

The preceding theory for the analysis of cavity-backed microstrip arrays is adapted in this section to the conventional arrangement of microstrip patch arrays on an infinite dielectric substrate (see Fig. 2). The procedure is based on the application of the waveguide simulator model (WGS), which reproduces the electromagnetic behavior of an infinite array in one or more periodic cells in a housing rectangular waveguide [19]. If a WGS is used to analyze an infinite microstrip array fed by a probe from a coaxial line placed on the ground plane, the initial radiating problem is converted into a physically bounded one. Fig. 3 shows the resultant structure for an array of circular patches. It can be considered as a transverse multidiscontinuity problem between different homogeneous waveguides of arbitrary cross sections, similar to the structure analyzed in Section II without the aperture discontinuity and ended in a matched rectangular waveguide. This computational model avoids building a new simulator for each frequency or scan angle and allows consideration of magnetic walls in order to extend the analysis to dual or circular polarization.

To validate this procedure, two different arrays have been analyzed. The first example (reported in [9]) is an infinite array of circular patches. The simulator is a standard S-band rectangular waveguide operating in the TE_{10} mode that simulates a scanning of the array in the H plane. In the reference, only the probe radius is specified and modeled. For our analysis, a semirigid coaxial model RG-.402/U (50 Ω) with the same inner radius has been chosen and all the dimensions and dielectric constant considered. The analysis

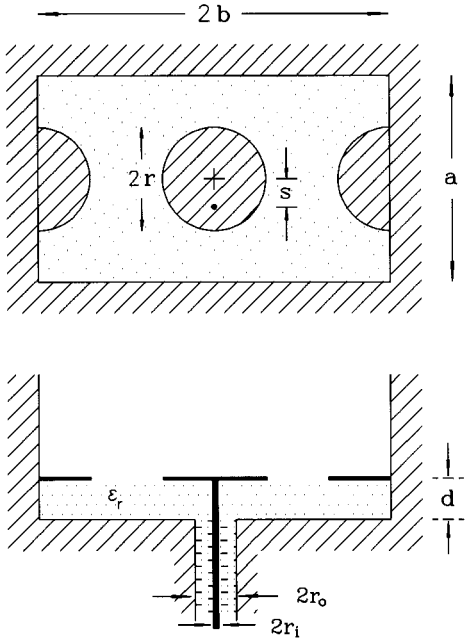

Fig. 3. Waveguide simulator for an infinite array of circular patches with coaxial feed ($r = 1.429$ cm; $s = 0.5$ cm; $a = 3.4$ cm; $2b = 7.22$ cm; $d = 0.079$ cm; $\epsilon_r = 2.33 \pm 0.02$; coaxial feed: $\epsilon_{rx} = 2.024$; $r_i = 0.456$ mm; $r_o = 1.492$ mm).

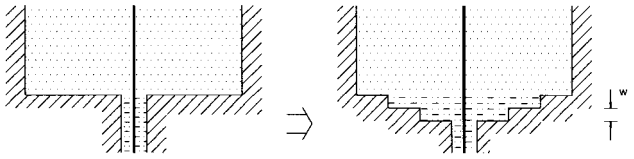

Fig. 4. Insertion of fictitious stepped sections of coaxial lines with very small or null lengths ($w \approx 0$) in the transition coaxial line substrate.

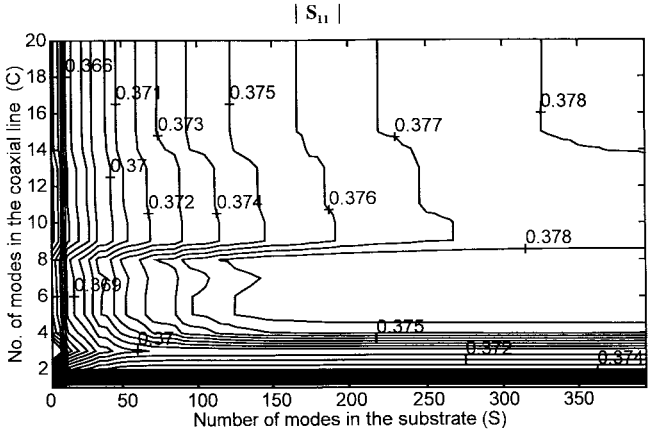

Fig. 5. Convergence study of the TEM mode-reflection coefficient (S_{11}) in the first coaxial line for the transition coaxial substrate solved with fictitious steps. The magnitude of S_{11} versus the number of modes S and C in the corresponding modal series is represented.

by the MM-GSM procedure of the kind of structure shown in Fig. 3 requires an appropriate ratio of number of modes at each discontinuity to obtain convergent results.

The asymmetric transition coaxial line-circular rectangular coaxial line (substrate geometry) is not solved directly because the notable size difference between their cross sections. This solution would lead to considering a very large number of modes in the substrate. The insertion of intermediate fictitious sections of coaxial lines with very small or null lengths and different outer radii (as shown in Fig. 4) allows reduction of the number of modes to be employed and enhancement accuracy avoiding numerical instabilities [20]. In Fig. 5, the convergence of the TEM mode-reflection coefficient for this transition, solved with two intermediate steps with zero length ($w = 0$), is illustrated. The graphs represent lines with the same magnitude of this parameter by varying the number of modes in the substrate (S) and coaxial lines. In the y axis, (C) represents the modes in the first coaxial and the number of modes in the fictitious sections are obtained by fixing the same angular variation in all of them and taking the radial variations equal to the ratio of radii for each single discontinuity. The figure shows a region from $S = 150$ with around $C = 7$ modes where the fluctuations are not significant. The same behavior has been observed for the equal-phase curves. For the step approach, convergent results are obtained with a smaller number of modes in the substrate than in the direct junction case where a greater modal ratio (substrate/coaxial) is required.

On the other hand, the small thickness of metal patches, which leads to closely separated discontinuities, may be a source of numerical instabilities. A study of the convergence behavior for the transitions substrate-patch-rectangular waveguide has been carried out by varying the number of modes in the regions corresponding to the substrate (M) and the patches (N), but assuming the same number of modes in the rectangular waveguide and the substrate because they have practically the same cross sections. The results in Fig. 6 represent the reflection coefficient for the TEM mode in the substrate at 4.1 GHz. Only the magnitude is shown in the figure, but a similar behavior is exhibited for the phase curves. It can be established that with a modal ratio (M/N) greater than 1.5 times the ratio of the respective cross sections R_a and from a threshold ($N \approx 25$) in the patch geometry, the figure shows a spacious region where the convergence is achieved. This behavior is similar to that reported in [21] for numerical methods involving equation systems that relate two truncated series. Numerical studies have stated that when the modal ratio exceeds a value, the results converge taking a sufficient number of terms in the modal series. We have found that this criterion gives good convergence in all studied geometries for this double transition.

Fig. 7 compares the results for the active reflection coefficient in [9] with our predictions. The agreement with the measured data was achieved in the reference and with the proposed technique by correcting the substrate permittivity from the nominal value $\epsilon_r = 2.33$ to 2.28 and 2.29, respectively. To illustrate the effect of the coaxial size, the analysis has been reproduced with different values of the outer radius and permittivity of the coaxial line, but retaining its initial characteristic impedance. The results in Fig. 8 show how the resonant frequency shifts down and the impedance matching changes lightly when the coaxial aperture is increased. This is due to the field alteration in the transition that must be taken into account when the coaxial dimensions are not negligible.

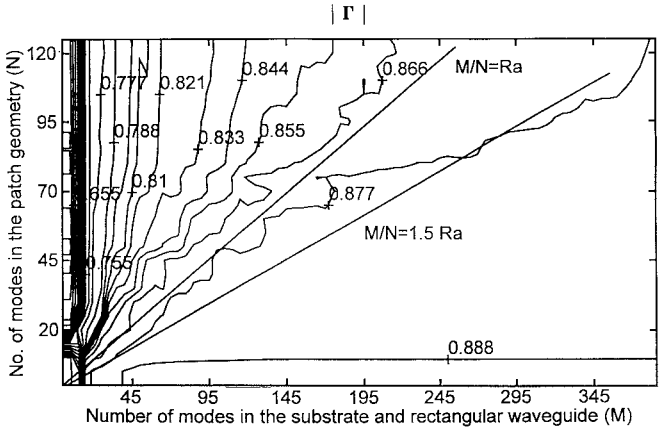

Fig. 6. Convergence study of the TEM mode reflection coefficient (Γ) in the substrate transmission line for the double transition substrate-patch-rectangular waveguide. The magnitude of Γ versus the number of modes M and N in the corresponding modal series is represented.

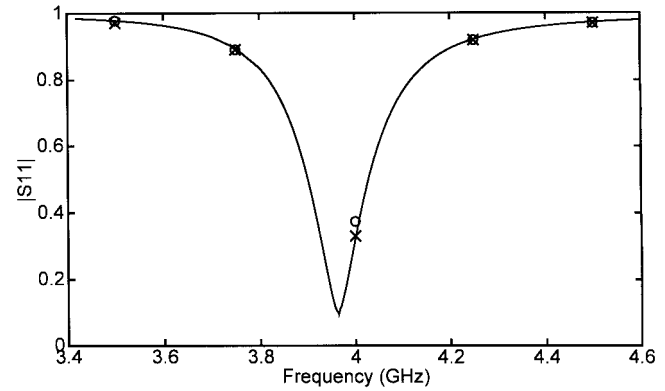

(a)

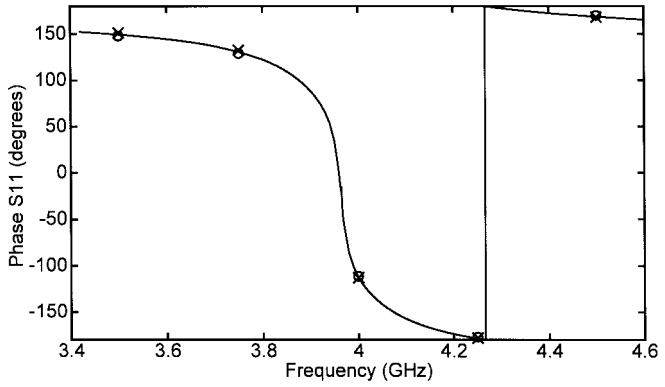

(b)

Fig. 7. Reflection coefficient (S_{11}) of the infinite array of circular patches in S-band waveguide simulator defined in Fig 3. (a) Magnitude. (b) Phase. ($\times$ $\times$): measured in [9]; (oo): simulated in [9] with $\epsilon_r = 2.28$; (—): simulated here with $\epsilon_r = 2.29$.

In the next example, an infinite array of square patches is considered. A prototype has been implemented and measured in a WGS, constituted by a matched standard C-band rectangular waveguide. The experiments were done on a tetrafluorethylen (PTFE) substrate. The patch element is fed by the center conductor of a SMA connector of 50 Ω. Fig. 9 presents the measured active reflection and transmission

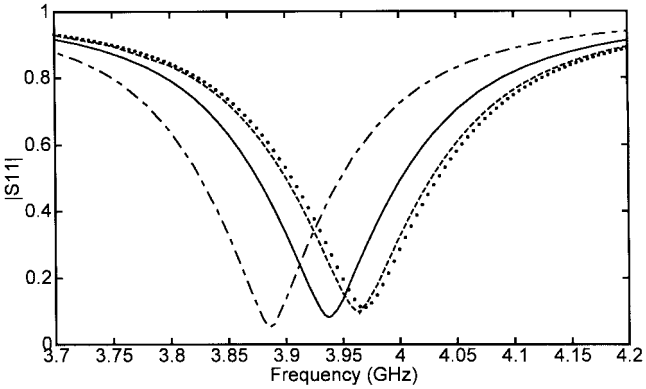

Fig. 8. Calculated reflection coefficient magnitude of the infinite array of circular patches in S-band waveguided simulator defined in Fig. 3 for varying the outer radius (r_o) of the coaxial feed line. (- - -): $r_o = 1.492$ mm; (•••): $r_o' = 0.7\ r_o$; (—): $r_o'' = 1.47\ r_o$; (— – —): $r_o''' = 2.25\ r_o$.

coefficients together with the results obtained by the method presented here. An excellent agreement has been achieved with a permittivity correction ($\epsilon_r = 2.61$) and substrate thickness ($d = 2.42$ mm), both inside the tolerances. The proposed technique allows accurate predictions not only for the resonant frequency, but also for the reflection coefficient values because the feed is modeled without approximations. The measures show a spurious resonant frequency at 4.85 GHz that is reproduced, however, like a total reflection in the simulation. The measured transmission coefficient from coaxial to rectangular waveguide indicates the loss dissipation at this frequency, which is not included in the theoretical model.

IV. Results of Cavity-Backed Arrays

To illustrate the usefulness of the full-wave method (developed in Section II) applied to the analysis of cavity-backed microstrip arrays, in this section, numerical results for the active reflection coefficient are compared with measurements in waveguide simulator. Scan performance results are also presented and compared with other numerical predictions. All conclusions obtained in Section III related to the ratio of modes selection have been applied now for analogous waveguide transitions. The ratio space harmonics modes employed to solve the rectangular aperture array half-space discontinuity is the ratio of areas between the periodic cell and the rectangular aperture in each case, [16].

The unit cell of the first considered array is depicted in Fig. 10. The substrate and feed coaxial line are the same as in the previous example and, therefore, the same corrected values of ϵ_{r1} and d are used. The measurements were performed with the same C-band waveguide simulator but now placed on only one periodic cell. In this way, the structure to be measured will be the unit cell in Fig. 10 ended with a matched rectangular waveguide with dimensions a and b in agreement with the array periodicity. This disposition models an infinite array excited to have a main and grating lobes radiating in opposite angles. Theoretical predictions assuming both WGS and infinite array are shown in Fig. 11, together with the measured active reflection coefficient. Two different

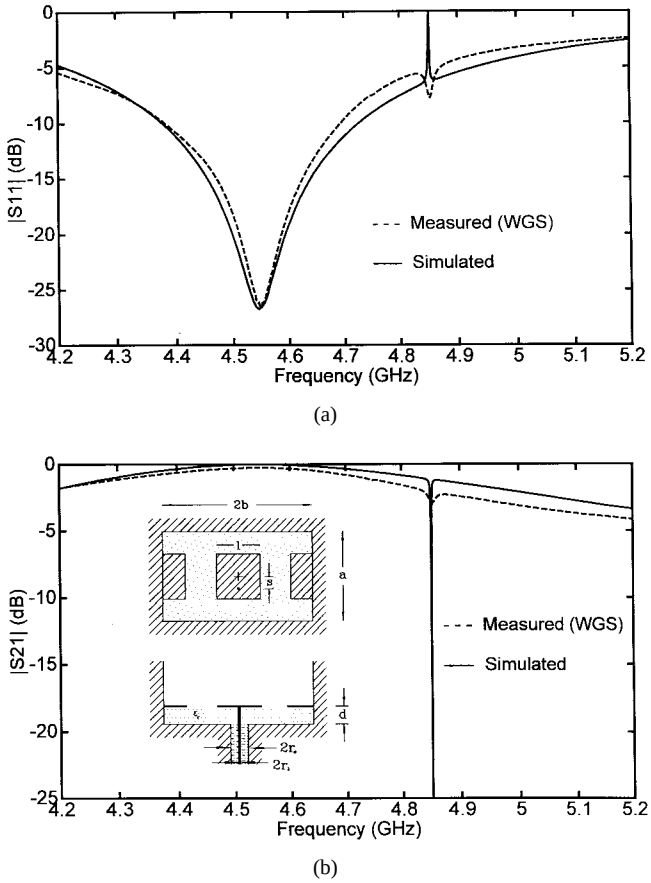

Fig. 9. Magnitude of the measured and calculated reflection (S_{11}) and transmission (S_{21}) coefficients of an infinite array of square patches in C-band waveguide simulator ($a = 2.215$ cm; $b = 2.378$ cm; $l = 1.8$ cm; $s = 0.48$ cm; $\epsilon_r = 2.58 \pm 0.04$; $d = 2.362$ mm $\pm$ 0.076; coaxial feed: $\epsilon_{rx} = 1.951$; $r_i = 0.64$ mm; $r_o = 2.05$ mm).

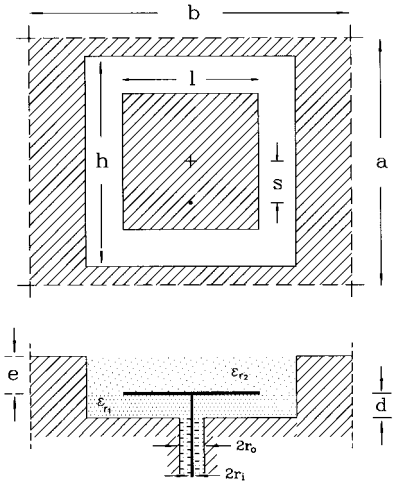

Fig. 10. Elementary cell of an infinite array of cavity-backed square patches fed by coaxial lines ($l = 1.35$ cm; $h = 1.815$ cm; $d = 2.362$ mm $\pm$0.076; $s = 1.75$ mm; $\epsilon_{r1} = 2.58 \pm 0.04$; $\epsilon_{r2} = 1.0$; $a = 2.215$ cm; b=4.756 cm; coaxial feed: $\epsilon_{rx} = 1.951$; $r_i = 0.64$ mm; $r_o = 2.05$ mm).

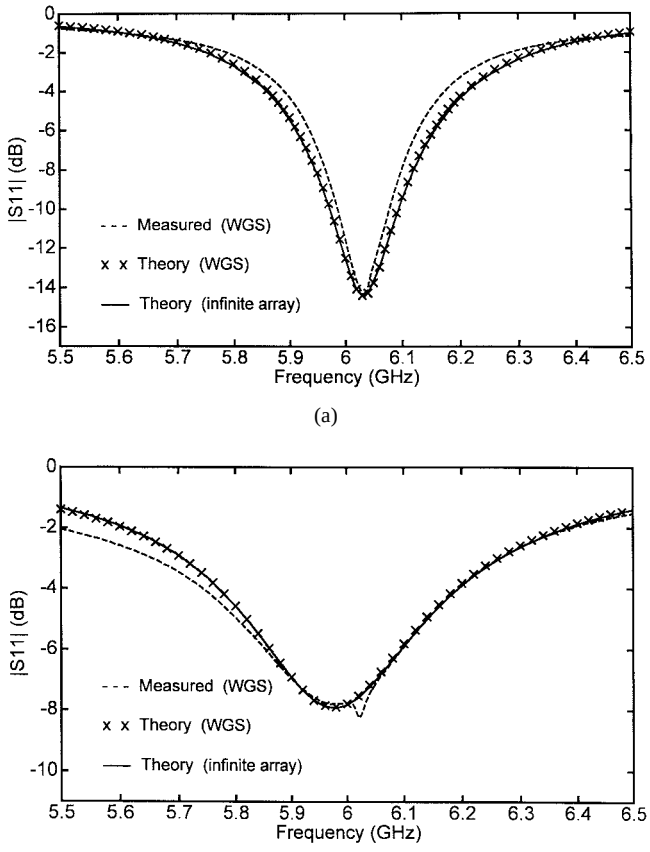

Fig. 11. Measured and simulated active reflection coefficient magnitude in C-band waveguide simulator of the infinite cavity-backed microstrip array defined in Fig. 10. Simulated with $\epsilon_{r1} = 2.61$, $d = 2.42$ mm. (a) $e = 2.6$ mm, $\epsilon_{r2} = 1.0$. (b) $e = 0$ mm.

situations are considered: 1) recessing the patches into the cavity ($e \neq 0$) and 2) with the convectional disposition of the patches and cavity aperture over the same plane ($e = 0$). The figure shows a practical coincidence between the WGS and array predictions. This fact validates the WGS as a suitable model for infinite arrays. Besides, in both cases measurements and predictions show a good agreement with some deviation attributable to losses and mechanic tolerances.

Results for an array with identical radiant elements, but with a new periodicity in x direction ($b = 2.378$ cm) are shown in Fig 12. The C-band WGS is placed now on two periodic cells. The comparison of Figs. 11(a) and 12(b) indicates that when the patches are recessed into the cavity the active reflection coefficient is practically the same for both periodicities. As it could be expected for this configuration, the array characteristics are determined fundamentally by the patch geometry into the cavity and not for the array configuration.

To illustrate the effect of the feed coaxial size in the scan performance, the broadside-matched active reflection coefficient of the former cavity-backed array has been computed for three different coaxial outer radii, maintaining the same characteristic impedance. The results in Fig. 13 show how the variation of the input impedance versus scan is altered. The E-plane scan performance is lightly deteriorated as the coaxial aperture increases. On the contrary, in the H plane it is clearly improved. The effect will be noticeable when the coaxial aperture is not negligible, for example it may appear for the use of microstrip antennas at millimeter frequencies.

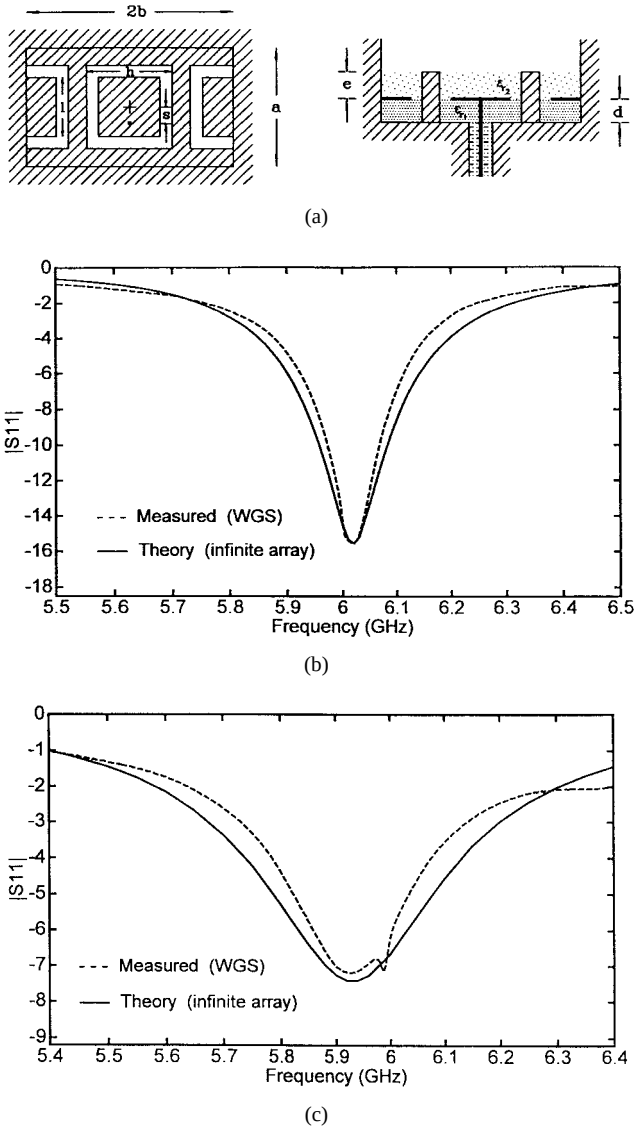

Fig. 12. Measured and calculated active reflection coefficient magnitude in C-band waveguide simulator of the infinite cavity-backed microstrip array described in Fig. 10, with $b = 2.378$ cm (simulated with $\epsilon_{r1} = 2.61$, $d = 2.42$ mm). (a) Measured structure. (b) Results with $e = 2.6$ mm, $\epsilon_{r2} = 1.0$. (b) Results with $e = 0$ mm.

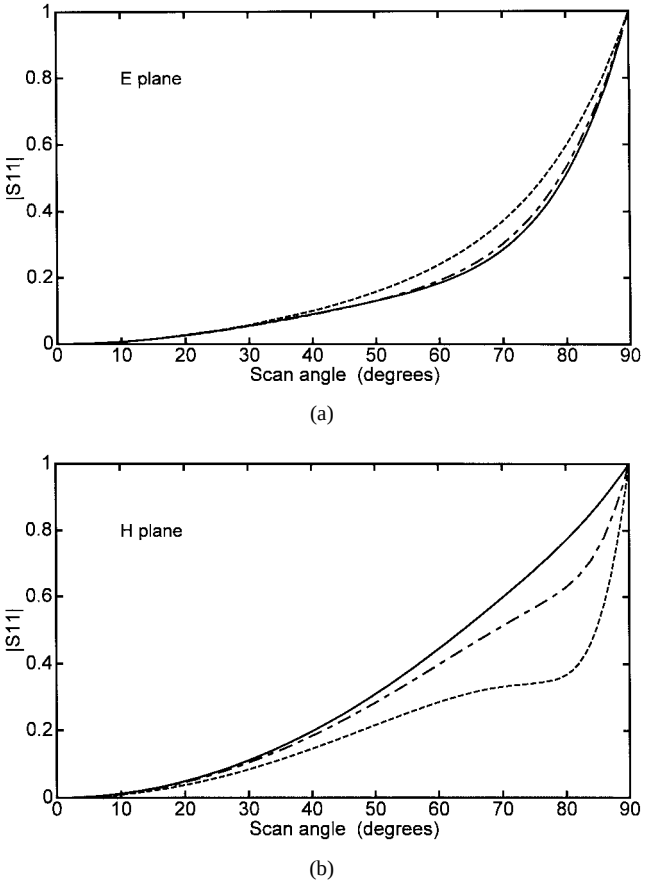

Fig. 13. Calculated magnitude of the broadside-matched active reflection coefficient versus the scan angle of the infinite cavity-backed microstrip array defined in Fig. 10 ($b = 2.378$ cm) for different outer radii of the coaxial feed line. (a) E plane. (b) H plane. (—): $r_o = 2.05$ mm; (— – —): $r_o' = 1.7 r_o$; (- - -): $r_o'' = 2.31\ r_o$.

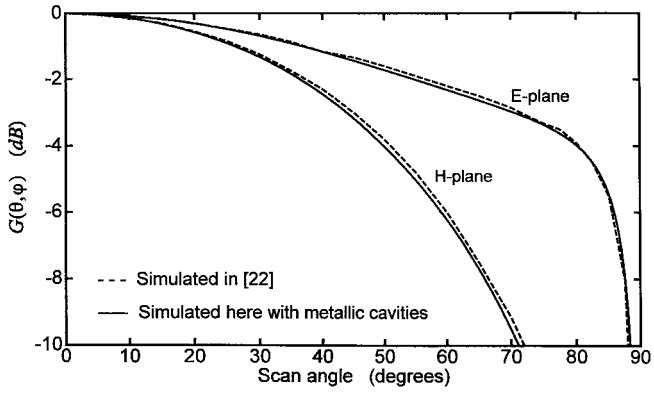

Fig. 14. Normalized active element pattern of the infinite array of rectangular microstrip patches described in Fig. 2.

The scan performance of a conventional microstrip array when thin substrates are employed ($d \leq 0.02\lambda_o$) is not very different to the same array of cavity-backed patches, as is demonstrated in [2] for circular patches and cavity cross sections. Based on this behavior, the active element pattern of an infinite array of conventional rectangular patches analyzed in [22] (see Fig. 2) with a substrate thickness of 0.003 λ_o has been reproduced with the technique proposed in Section II after inserting thin metallic walls between the adjacent cells of the array. The results for E and H planes are depicted in Fig. 14 at 1.21 GHz and a very good agreement with numerical results in the reference is observed.

V. Conclusion

A hybrid MM-GSM-FE numerical technique for the analysis of infinite arrays of microstrip patches with arbitrary geometry and backed by metallic cavities has been presented in this paper. The method is combined with the waveguide simulator concept to analyze conventional arrays on an infinite dielectric substrate. To validate the analysis procedure, it has been applied to the characterization of different infinite arrays with circular, square, and rectangular patches. Results including active reflection coefficients and active element patterns have been obtained and compared with measurements from prototypes implemented on waveguide simulator and other

experimental and theoretical data available in the literature. The proposed method provides a rigorous characterization of the coaxial feed and allows accurate predictions of the active input impedance, particularly in the analysis of cavity-backed arrays involving thick substrates and/or coaxial feed with nonnegligible dimensions, where other methods fail. In contrast to other 3-D numerical techniques, a more efficient 2-D FEM combined with the MM technique is used to analyze the coaxial feed and cavity region.

APPENDIX

If $\vec{e}_n^{\,j}$ and $\vec{h}_m^{\,i}$ in (5) are expressed as a function of the derivatives of the axial field components A_z for TE and TM modes and the scalar electric potential Φ for TEM modes, the coupling integrals may be expressed in a general form as

$$X(n,m) = \sum_{l=1}^{L} \int_{S_{c_l}} F\left(\frac{\partial \psi_n^j}{\partial p}, \frac{\partial \psi_n^j}{\partial q}, \frac{\partial \chi_m^i}{\partial p}, \frac{\partial \chi_m^i}{\partial q}\right) dS \quad (6)$$

where ψ and χ represent E_z, H_z or Φ according to the different modal combination possibilities in (3), and (p, q) are the transversal local coordinates. A Gauss quadrature rule for the numerical computation of these integrals may be applied because of coherent meshes are employed. In this way, (6) may be expressed as

$$X(n,m) = \sum_{l=1}^{L} \left[\sum_{k=1}^{K} W_k \cdot F\left(\frac{\partial \psi_n^j}{\partial p}, \frac{\partial \psi_n^j}{\partial q}, \frac{\partial \chi_m^i}{\partial p}, \frac{\partial \chi_m^i}{\partial q}\right)\Big|_{(p_k, q_k)} \right]_l \quad (7)$$

where (p_k, q_k) and W_k are the integration points and the corresponding weights, respectively.

For canonical waveguides, analytical expressions of ψ^j and χ^i may be employed to compute (7) but numerical solutions must be obtained for any other arbitrarily shaped homogeneous waveguides.

To obtain a numerical mode representation, the FEM is used for the discretization with second order quadrangular and triangular isoparametric elements of Lagrange kind of the associated functionals for scalar Helmholtz and Laplace equations. These functionals are known to be

$$F(A_z) = \frac{1}{2} \int_S \left[(\nabla_t A_z)^2 - k_c^2 A_z^2 \right] ds \quad (8a)$$

and

$$F(\Phi) = \frac{1}{2} \int_S \varepsilon (\nabla_t \Phi)^2 ds \quad (8b)$$

for TE and TM modes (where k_c is the cutoff wave number) and for TEM modes, respectively. The formulation (8a) leads to an eigenvalue problem of the form

$$[K]\{A_z\} = -\beta^2 [M]\{A_z\} \quad (9)$$

where $\{A_z\}$ are column matrices containing the values of A_z in the nodes of the mesh and β is the phase constant. This eigensystem is solved by the subspace iteration method, composed of a sequence of inverse iterations and Rayleight Ritz analysis on each subspace. The eigenvalues and eigenvectors in this subspace are calculated by the generalized Jacobi method [23].

REFERENCES

[1] D. M. Pozar, "Microstrip antennas," *Proc. IEEE*, vol. 80, pp. 79–91, Jan. 1992.

[2] F. Zavosh and J. T. Aberle, "Infinite phased arrays of cavity-backed patches," *IEEE Trans. Antennas Propagat.*, vol. 42, pp. 390–398, Mar. 1994.

[3] M. Davidovitz, "Extension of *E*-plane scanning range in large microstrip arrays by substrate modification," *IEEE Microwave Guided Wave Lett.*, vol. 2, pp. 492–494, Dec. 1992.

[4] J. M. Jing and L. Volakis, "A hybrid finite element method for scattering and radiation by microstrip patch antennas and arrays residing in a cavity," *IEEE Trans. Antennas Propagat.*, vol. 39, pp. 1598–1604, Nov. 1991.

[5] J.-C. Cheng and L. P. B. Katehi, "Theoretical modeling of cavity-backed patch antennas using a hybrid technique," *IEEE Trans. Antennas Propagat.*, vol. 43, pp. 1003–1013, Sept. 1995.

[6] J. Gong and J. L. Volakis, "An efficient and accurate model of the coax cable feeding structure for FEM simulations," *IEEE Trans. Antennas Propagat.*, vol. 43, pp. 1474–1478, Dec. 1995.

[7] D. M. Pozar and D. H. Schaubert, "Analysis of an infinite array of rectangular microstrip patches with idealized probe feeds," *IEEE Trans. Antennas Propagat.*, vol. 32, pp. 1101–1107, Oct. 1984.

[8] J. T. Aberle and D. M. Pozar, "Analysis of infinite arrays of rectangular microstrip patches using a rigorous feed model," *Proc. Inst. Elect. Eng.*, vol. 136, no. 2, pp. 110–119, Apr. 1989.

[9] ——, "Analysis of infinite arrays of one and two-probe-fed circular patches," *IEEE Trans. Antennas Propagat.*, vol. 38, pp. 421–432, Apr. 1990.

[10] R. C. Hall and J. R. Mosig, "The analysis of coaxially fed microstrip antennas with electrically thick substrates," *J. Electromagn. Waves Applicat.*, vol. 9, pp. 367–384, 1989.

[11] M. Davidovitz and Y. T. Lo, "Input impedance of a probe-fed circular microstrip antenna with thick substrate," *IEEE Trans. Antennas Propagat.*, vol. 34, pp. 905–911, July 1986.

[12] A. Das and S. K. Das, "Input impedance of a probe excited circular microstrip ring antenna," *Proc. Inst. Elect. Eng.*, vol. 132, no. 6, pp. 384–390, Oct. 1985.

[13] C. Wu, K. L. Wu, Z. Bi, and J. Litva, "Modeling of coaxial-fed microstrip patch antenna by finite difference time domain method," *Electron. Lett.*, vol. 27, no. 19, pp. 1691–1692, Sept. 1991.

[14] J. Zapata and J. García, "Analysis of passive microwave structures by a combined finite element generalized scattering matrix method," in *Proc. North American Radio Sci. Meet.*, London, ON, Canada, June 1991, vol. 1, p. 146.

[15] J. Zapata, J. García, L. Valor, and J. M. Garai, "Field-theory analysis of cross-iris coupling in circular waveguide resonators," *Microwave Opt. Technol. Lett.*, vol. 6, no. 16, pp. 905–907, Dec. 1993.

[16] M. Lambea and J. A. Encinar, "Analysis of multilayer frequency selective surfaces with rectangular geometries," presented at *9th Int. Conf. Antennas Propagat.*, Eindhoven, The Netherlands, 1995.

[17] M. Lambea, M. A. González, J. A. Encinar, and J. Zapata, "Analysis of FSS with arbitrarily shaped apertures by finite element method and generalized scattering matrix," presented at *IEEE Int. Antennas Propagat. Symp.*, Newport Beach, CA, June 1995.

[18] R. C. Hansen, Ed., *Microwave Scanning Antennas*. New York: Academic, 1966.

[19] P. W. Hannan and M. A. Balfour, "Simulation of phased-array antennas in waveguides," *IEEE Trans. Antennas Propagat.*, vol. AP-13, pp. 342–353, May 1965.

[20] U. Papziner and F. Arnt, "Field theorerical computer-aided design of rectangular and circular iris coupled rectangular or circular waveguides cavity filters," *IEEE Trans. Microwave Theory Tech.*, vol. 41, pp. 462–471, Mar. 1993.

[21] R. Sorrentino, M. Mongiardo, F. Alessandri, and Schiavon, "An investigation of the numerical properties of the mode-matching technique," *Int. J. Numer. Modeling: Electron. Networks, Devices, Fields*, vol. 4, pp. 19–43, Mar. 1991.

[22] A. K. Skrivervik and J. R. Mosig, "Finite phased array of microstrip patch antennas: The infinite array approach," *IEEE Trans. Antennas Propagat.*, vol. 40, pp. 579–592, May 1992.

[23] K. J. Bathe and E. L. Wilson, *Numerical Methods in Finite Element Analysis*. Englewood Cliffs, NJ: Prentice-Hall, 1976, pp. 494–506.

Miguel A. González de Aza was born in Madrid, Spain. He received the Ing. Telecomunicación and Ph.D. degrees from the Universidad Politécnica de Madrid, Spain, in 1989 and 1997, respectively.

From 1990 to 1992, he has been with the Departamento de Electromagnetismo y Teoría de Circuitos at the Universidad Politécnica de Madrid on a research scholarship from the Spanish Ministry of Education and Science. He became an Assistant Professor and an Associate Professor in 1992 and 1997, respectively, at the same university. His main research interests include analytical and numerical techniques for the analysis and characterization of waveguide structures and microstrip antennas.

José A. Encinar (S'81–M'86) was born in Madrid, Spain, in 1957. He received the Ing. Telecomunicación and Ph.D. degrees both from Universidad Politécnica de Madrid, in 1979 and 1985, respectively.

He has been with the Grupo de Electromagnetismo Aplicado y Microondas at the Universidad Politécnica de Madrid as a Teaching and Research Assistant from 1980 to 1982 and as an Assistant Professor from 1983 to 1986. In 1986 he became an Associate Professor at the same university. From February to October of 1987 he was with the Polytechnic University, Brooklyn, NY, as Post-Doctoral Fellow of the NATO Science Program. He is currently a Professor of Electromagnetism and Circuit Theory Department at the Universidad Politécnica de Madrid. His research interests include analytical and numerical techniques for the analysis and design of waveguide structures, frequency selective surfaces, and radiating systems.

Juan Zapata (M'93) received the Ing. Telecomunicación and the Ph.D. degrees, in 1970 in 1974, respectively, from the Universidad Politécnica de Madrid, Spain.

He has been with the Departamento de Electromagnetismo y Teoría de Circuitos at the Universidad Politécnica de Madrid since 1970, first as an Assistant Professor, then an Associate Professor in 1975, and a Professor in 1983. He has been engaged in research on microwave active circuits and interactions of electromagnetic fields with biological tissues. His current research interest include computer-aided design for microwave passive circuits and numerical methods in electromagnetism.

Manuel Lambea (M'95) was born in Badajoz, Spain, in 1963. He received the Ing. Telecomunicación and Ph.D. degrees from the Universidad Politécnica de Madrid, in 1989 and 1996, respectively.

From October 1989 to September 1990, he was with the Grupo de Ingeniería de Comunicaciones at the Universidad de Málaga as an Assistant Professor. From 1990 to 1996 he was with the Electromagnetism and Circuit Theory Department at the Universidad Politécnica de Madrid as an Assistant Professor. In October 1996 he became an Associate Professor. His research interests include frequency selective surfaces and radiating systems and analytical and numerical techniques for the analysis and design of waveguide structures.